NIRCam Optical Analysis

Yalan Mao, Lynn W. Huff and Zachary A. Granger
Lockheed Martin Advanced Technology Center, 3251 Hanover St., Palo Alto, CA 94304

ABSTRACT

The Near Infrared Camera (NIRCam) instrument for NASA's James Webb Space Telescope (JWST) is one of the four science instruments to be installed into the Integrated Science Instrument Module (ISIM) on JWST. NIRCam's requirements include operation at 37 Kelvin to produce high-resolution images in two wave bands encompassing the range from 0.6 microns to 5 microns. In addition, NIRCam is to be used as a metrology instrument during the JWST observatory commissioning on orbit, during the precise alignment of the observatory's multiple-segment primary mirror. This paper will present the optical analyses performed in the development of the NIRCam optical system. The Compound Reflectance concept to specify coating on optics for ghost image reduction is introduced in this paper.

Key words: NIRCam, JWST, Compound Reflectance, Optical analysis, ghost image

1. INTRODUCTION

NIRCam is a science instrument that will make up part of the science instrument complement of the James Webb Space Telescope (JWST). The JWST will possess a large aperture of 6.5m with several times the collecting area of the Hubble Space Telescope. JWST will have a broadband IR capability that, from the vicinity of Lagrange 2 (nine hundred thousand km from earth), will allow a view into the distant history of galaxy formation. The instrument will be required to furnish high-quality infrared imaging performance while operating in a challenging cryogenic (32 - 37 Kelvin) space environment over a minimum 5-year (10 year goal) mission.

The NIRCam Instrument consists of two identical/symmetrical Modules (A and B) that are mounted back to back symmetrical about the V2 axis[1]. Each module is required to image a different part of the OTE (Optical Telescope Element) field of view. The spectral band is 0.6 microns to 5.0 microns, with a transition zone between 2.3 and 2.4 microns. Each Module consists of a Shortwave (λ = 0.6 to 2.3 microns) Imager and Coronagraph, and a Longwave (λ = 2.4 to 5.0 microns) Imager and Coronagraph. The Imaging mode of each Module has a square field of view of 2.2 arcmin on a side. The instrument will be mounted to the ISIM (Integrated Science Instrument Module) of the spacecraft via kinematics' mounts.

In this paper, we will present the vignetting analysis, alignment sensitivity analysis and ghost image analysis. In the ghost analysis, we have introduced the Compound Reflectance concept for specifying coating reflectance on both sides of an optical element when ghost image is a concern.

2. NIRCam OPTICAL LAYOUT

Layouts of the NIRCam optical paths are shown in Figure 1. The table in Figure 1 describes the naming convention for the various NIRCam optical elements.

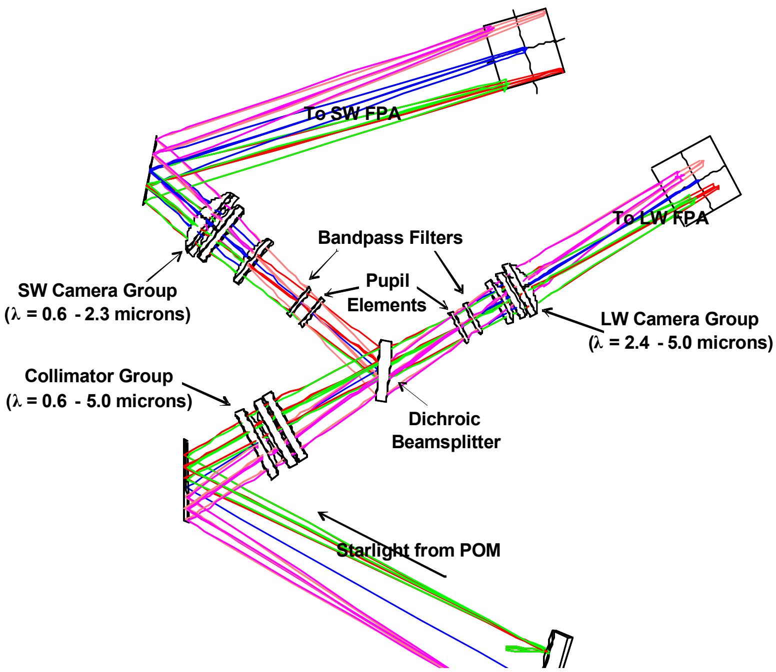

Element		Designation
Common Path		
Pickoff Mirror		POM
Coronagraphic Occulting Mask		COM
First Fold Mirror		FFM
First (ZnSe) Collimator Lens		Col1
Second (BaF2) Collimator Lens		Col2
Third (LiF) Collimator Lens		Col3
Dichroic Beamsplitter		DBS
Shortwave Path		
Shortwave Pupil Elements		SWP
Shortwave Filters		SWF
First (LiF) Shortwave Camera Lens		SW1
Second (BaF2) Shortwave Camera Lens		SW2
Third (ZnSe) Camera Shortwave Lens		SW3
Shortwave Fold Flat		SWFF
Shortwave FPA Flat		SWFPA Flat
Shortwave FPA		SWFPA
Longwave Path		
Longwave Pupil Elements		LWP
Longwave Filters		LWF
First (LiF) Longwave Camera Lens		LW1
Second (BaF2) Longwave Camera Lens		LW2
Third (ZnSe) Longwave Camera Lens		LW3
Longwave FPA Flat		LWFPA Flat
Longwave FPA		LWFPA

Figure 1: NIRCam Optical Layout

3. VIGNETTING ANALYSIS

3.1. Approach for Vignetting Analysis

The modeling was done using ZEMAX[2] optical design and analysis software. In all cases, the Imaging path was modeled using five field points (the center point and the four corners), and the Coronagraphic path was modeled using seven points. The relative location of the various field points is shown in Figure 2.

The modeling was not done on NIRCam as a stand-alone system, but rather incorporated the JWST Optical Telescope Element (OTE) to create an end-to-end integrated system (see a footprint example of segment primary mirror[3] in Figure 3). For reasons of modeling simplicity, the entrance pupil of JWST was assumed to be a circle circumscribing the irregular shape of the OTE Primary Mirror. As a result, our modeling starts with a nominal geometrical throughput of 71.60%, or a 28.4% loss due to obscurations at the OTE primary mirror. These obscurations include the central obscuration and obscurations from the gaps/edges of the hexagonal segments. Therefore, within the context of this analysis, a throughput of 71.60% (as shown in the "% RAYS THROUGH =" in the lower right of Figure 2 and 3) indicates that no light has been vignetted within NIRCam.

3.2. Vignetting Analysis Results and Summary

The footprints of starlight through NIRCam from the various field points are compared with the nominal sizes of the optics. The amount of vignetting has been analyzed for the Imaging and Coronagraphic paths. The results show that there is no vignetting in the Imaging paths, and slight vignetting in Coronagraphic paths. In imaging mode, NIRCam also meets the requirement for overfilling the active areas of the Focal Plane Assemblies.

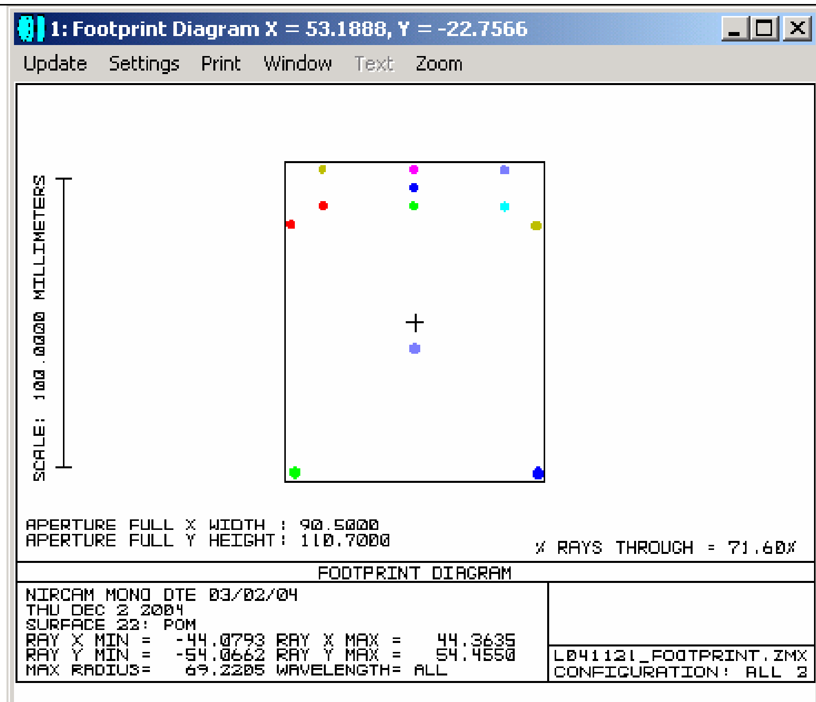

Figure 2: Location of various field points

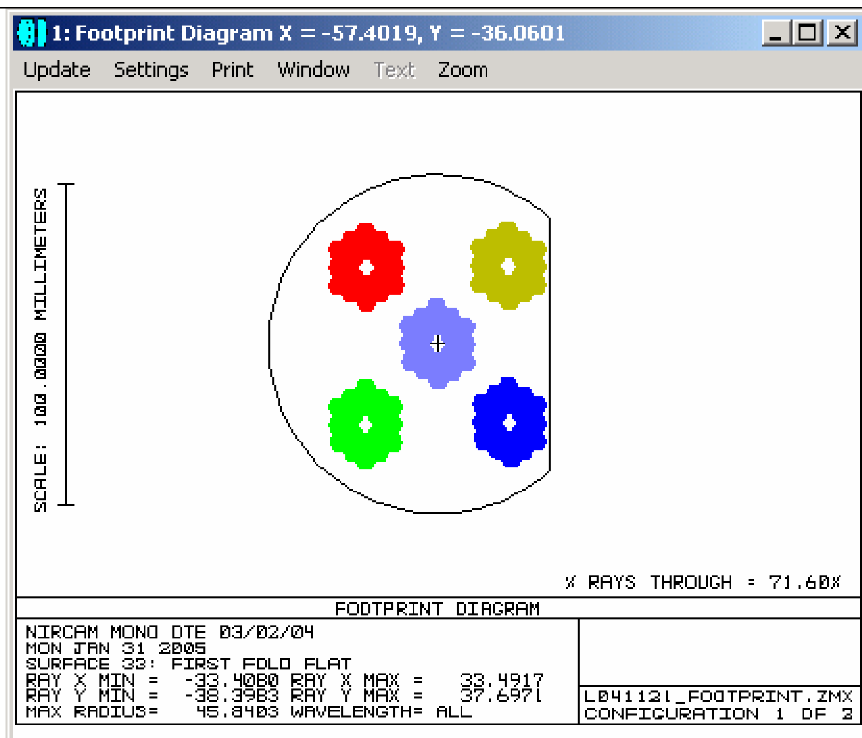

Figure 3: Image field points at First Fold Flat assemble segmented Primary Mirror

4. ALIGNMENT SENSITIVITY ANALYSIS

4.1. Approach for Sensitivity Analysis

The alignment sensitivity analysis was done using the Zemax optical design software. The approach to the analysis was as follows:

1. Beginning with the nominal NIRCam optical design, each optic was individually perturbed a prescribed amount in each degree of freedom (DOF). For most optics, the perturbations that were modeled were lateral displacement, angular rotation, and longitudinal displacement, referred to as “decenter”, “tilt”, and “defocus”, respectively.
2. The change in the system image quality was then evaluated at three representative wavelengths. An example of the Zemax output (for the second Collimating Lens) is shown below:

Type	Surface		Field	Value	0.8um Change (nm)	1.4um Change (nm)	2.3um Change (nm)	Alignment Sensitivity (nm/mm)
TEDX	48	49	All	-0.05	0.74	0.68	0.56	13.2

3. Dividing the change in the WFE by the magnitude of the perturbation yields the Alignment Sensitivity for that optic in that DOF. For example, decentering the second Collimator Lens 0.050 mm resulted in an average increase in the system WFE of 0.66 nm rms, and the resultant Alignment Sensitivity is therefore (0.66 / 0.050 =) 13.2 nm/mm.
4. The Alignment Sensitivity for each optic was then multiplied by the alignment tolerance assigned to that optic for that DOF. The specified alignment tolerances are satisfied based on the definition in the NIRCam Optics & Mounts Subsystem Specification.
5. A table was then created, listing the Alignment Sensitivities of each optic, and their prescribed tolerances in each DOF. The results were summed in an rss fashion, and the total is entered into the Wavefront Error Budget as the “Alignment” term.

4.2. Shortwave Channel Results

The matrix that describes alignment errors for the NIRCam Shortwave channel is shown in Table 1.

SHORTWAVE SENSITIVITY ANALYSIS RESULTS: REFOCUS OF FPA ALLOWED (nm rms)							
	TOLERANCES			SENSITIVITY			Totals
Component	Decenter Tolerance (mm)	Tip/Tilt Tolerance (degree)	Defocus Tolerance (mm)	Sensitivity to Decenter (nm rms / mm)	Sensitivity to Tip/Tilt (nm rms / degree)	Sensitivity to Defocus (nm rms / mm)	Total WFE (nm rms)
POM	0.0500	0.0167		0.1	2.4	0.0	0.0
POM-FFF			0.0500	0.0	0.0	0.6	0.0
FFF	0.5000	0.0667		0.0	0.9	0.0	0.1
FFF-COL			0.5000	0.0	0.0	0.4	0.2
COL	0.0500	0.0167		5.8	31.9	0.0	0.6
COL1	0.0500	0.0167	0.0500	0.6	3.5	0.0	0.1
COL1-COL2			0.0500	0.0	0.0	0.1	0.0
COL2	0.0500	0.0167		13.2	9.8	0.0	0.7
COL2-COL3			0.0500	0.0	0.0	0.5	0.0
COL3	0.0500	0.0167		0.1	0.8	0.0	0.0
COL3-DBS			0.5000	0.0	0.0	2.2	1.1
DBS	0.2500	0.0667		0.0	11.5	0.0	0.8
DBS-SWF			0.5000	0.0	0.0	2.1	1.0
SWF	0.5000	0.0667		0.0	0.1	0.0	0.0
SWF-SW			0.5000	0.0	0.0	0.6	0.3
SW	0.2500	0.0667		1.0	7.9	0.0	0.6
SW1	0.0500	0.0167		11.1	15.5	0.0	0.6
SW1-SW2			0.0500	0.0	0.0	0.6	0.0
SW2	0.0500	0.0167		269.3	56.2	0.0	13.5
SW2-SW3			0.0500	0.0	0.0	0.4	0.0
SW3	0.0500	0.0167		164.1	89.4	0.0	8.3
SW3-SWFF			0.5000	0.0	0.0	0.0	0.0
SWFF	0.5000	0.0667		0.0	0.0	0.0	0.0
SWFF-SWFPAFlat			0.5000	0.0	0.0	0.0	0.0
SWFPAFlat	0.5000	0.0667		0.0	0.0	0.0	0.0
SWFPAFlat-FPA			0.5000	0.0	0.0	0.0	0.0
							16.0

Table 1: Shortwave Sensitivity Matrix

4.3. Longwave Channel Results

The matrix that describes alignment errors for the NIRCam Longwave channel is shown in Table 2.

LONGWAVE SENSITIVITY ANALYSIS RESULTS: REFOCUS OF FPA ALLOWED (nm rms)							
	TOLERANCES			SENSITIVITY			
Component	Decenter Tolerance (mm)	Tip/Tilt Tolerance (degrees)	Defocus Tolerance (mm)	Sensitivity to Decenter (nm rms / mm)	Sensitivity to Tip/Tilt (nm rms / degree)	Sensitivity to Defocus (nm rms / mm)	Totals (nm rms)
POM	0.050	0.0167		0.2	6.0	0.0	0.1
POM-FFF			0.500	0.0	0.0	1.0	0.5
FFF	0.500	0.0667		0.0	1.4	0.0	0.1
FFF-COL			0.500	0.0	0.0	0.6	0.3
COL	0.050	0.0167		2.3	7.5	0.0	0.2
COL1	0.050	0.0167		0.9	2.0	0.0	0.1
COL1-COL2			0.050	0.0	0.0	0.2	0.0
COL2	0.050	0.0167		4.9	4.4	0.0	0.3
COL2-COL3			0.050	0.0	0.0	3.1	0.2
COL3	0.050	0.0167		0.1	0.6	0.0	0.0
COL3-DBS			0.500	0.0	0.0	2.7	1.3
DBS	0.500	0.0667		0.0	0.3	0.0	0.0
DBS-LWF			0.500	0.0	0.0	2.7	1.3
LWF	0.050	0.0667		0.0	0.1	0.0	0.0
LWF-LW			0.500	0.0	0.0	2.7	1.3
LW	0.250	0.0667		1.8	2.1	0.0	0.5
LW1	0.050	0.0167		58.2	4.7	0.0	2.9
LW1-LW2			0.050	0.0	0.0	8.7	0.4
LW2	0.050	0.0167		326.5	38.1	0.0	16.3
LW2-LW3			0.050	0.0	0.0	103.1	5.2
LW3	0.050	0.0167		127.9	23.7	0.0	6.4
LW3-LWFPAFlat			0.500	0.0	0.0	4.2	2.1
LWFPAFlat	0.500	0.0667		0.0	0.0	0.0	0.0
LWFPAFlat-FPA			0.500	0.0	0.0	0.1	0.1
							18.8

Table 2: Longwave Sensitivity Matrix

4.4. Summary of Alignment Sensitivity Analysis

The NIRCam instrument can be built and operated with reasonable and realizable alignment tolerances. The overall increase in the NIRCam Wavefront Error (WFE) due to misalignments amounts to 16.0 nm rms (out of a budget of 70 nm rms[4]) in the Shortwave channel, and 18.8 nm rms (out of a budget of > 120 nm rms[4]) in the Longwave channel. The final two lenses in the two Camera Groups are sensitive to misalignment, particularly in decenter. A significant effort was made by the optical design team to minimize this sensitivity.

5. GHOST IMAGE ANALYSIS

5.1. Approach for Ghost Image Analysis

The ghost image analysis is performed with Zemax software to verify that the NIRCam optical system is compliant with the ghost image requirement, as follows: "No ghost images in the Optics Subsystem shall have a point spread function smaller than 1 arcsec in diameter, unless the ghost image is spatially coincident with the observed image, or its integrated flux is less than 1% of the observed image flux". Double bounce is assumed in the analysis. The optical transmission or reflection of the element is based on the preliminary coating design as following:

(1). Mirror coating is gold.
(2). Beam splitter has 95% reflectance at shortwave, 95% transmittance at longwave for Dichroic coating, 2% AR coating at longwave for the other surface.
(3). The average reflectance per lens surface is given in Table 3.

Group	Lens Material		
Collimator	ZnSe	BaF2 (uncoated)	LiF (uncoated)
	0.016744	0.0353508	0.024415147
SW Camera	ZnSe	BaF2	LiF
	0.011062	0.009494123	0.009451069
LW Camera	ZnSe	BaF2	LiF
	0.002026	0.002685818	0.002685818

Table 3: Reflectance of Each Lens Group and Lens Material

(4). Compound Reflectance is introduced for the coating reflectance requirement of bandpass filter in order to reduce the ghost image at focal plane. The Compound Reflectance of a bandpass filter is defined as the product of reflectance of side S1 and S2. For example, if side S1 reflectance is 10% and side S2 reflectance is 4%, then the compound reflectance is 0.4%. Each filter has total transmission requirement depending on the type of filters. In order to reduce the ghost image from the double bounce of two surfaces of filter, the reflectance of each surface needs to be specified for minimum double reflection. The relationship of Compound Reflectance with reflectance of each surface is listed below in Table 4 assuming the total transmittance 85%. The lower the Compound Reflectance is the better the system is.

R1	Tot T	R2	Compound Reflectance
0.01	0.85	0.141414	0.001414
0.02	0.85	0.132653	0.002653
0.03	0.85	0.123711	0.003711
0.04	0.85	0.114583	0.004583
0.05	0.85	0.105263	0.005263
0.06	0.85	0.095745	0.005745
0.07	0.85	0.086022	0.006022
0.08	0.85	0.076087	0.006087
0.09	0.85	0.065934	0.005934
0.1	0.85	0.055556	0.005556
0.11	0.85	0.044944	0.004944
0.12	0.85	0.034091	0.004091
0.13	0.85	0.022989	0.002989
0.14	0.85	0.011628	0.001628
0.15	0.85	0.000000	0.000000

Table 4: Filter Compound Reflectance, R1 (first surface reflectance) and R2 (second surface reflectance).

(5). Detector reflectance is ~12.1% average at shortwave, ~7.2% average at longwave. We show in the section 5.2 below that ghost image from the detector reflection is negligible. The detector becomes the scattering source for the stray light in the system.

In the NIRCam optical system, we have six lenses, filter, dichroic beam splitter and detector. The total number of optical surfaces to be considered in the ghost image analysis is 15 for shortwave, and 17 for longwave. The potential ghost images would be 15x14/2=105 for shortwave, 17x16/2=136 for longwave. However, it is not necessary to analyze all the ghost images. The screening technique is used based on the ghost image size and magnitude. The ghost magnitude is calculated in the form of relative ghost magnitude, which is the transmitted ghost energy per pixel to transmitted image energy per pixel at nominal situation.

5.2. Ghost Image Analysis Results

The ghost image formation is categorized in five different cases with examples as shown in Figure 4. The strongest ghost images are evaluated and the NIRCam refractive optical system is shown to meet the ghost image requirement.

Case1: the ghost image is focused at the focal plane assembly (FPA) with most of the rays getting through the system. An example of Case 1 is shown in Figure 4 Case 1. Case 1a shows the ghost reflection from SWFB and then SWFA in Figure 4. The ghost image formed at the FPA is focused (see Figure 4 case 1b), with most of rays getting through the system.

Case 2: the ghost image is focused, but outside of FPA. An example is shown in Figure 4 Case 2. The ghost reflection is off the SWFB, then the SWPA (see Figure 4 Case 2a). With four degrees tilt of the filter, the ghost image is focused outside of the FPA (see Figure 4 Case 2b). This example demonstrates the four degrees tilt of filter will eliminate the ghost images from filter surfaces to pupil surfaces.

Case 3: the ghost image is not well focused at the FPA, with partial ray getting through the system. An example of this category is shown in Figure 4 Case 3. The ghost reflection is off COL3B then COL2B.

Case 4: the ghost image is not focused at FPA, with a small number of rays getting through the system. An example is shown in Figure 4 Case 4. The ghost reflection is off SW2B then SW1B.

Case 5: the ghost image is reflected off the detector surface, and then bounced back from other surfaces. One of the most severe examples in this category is shown in Figure 4 Case 5. The ghost reflection is off detector surface (see Figure 4 Case 5a) then first surface of second lens in camera group (see Figure 4 Case 5b). The center field spot size is large; four corner fields are outside of the FPA (see Figure 4 Case 5c). The effect of the ghost images on the FPA is negligible in this example as well as in all the other ghost images in this category.

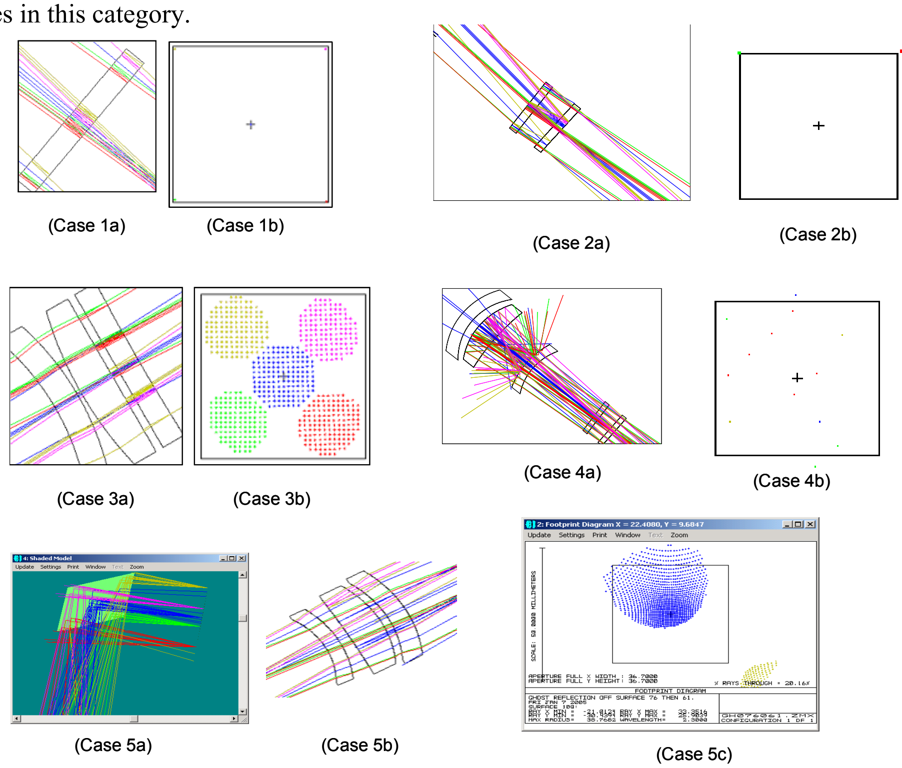

Figure 4: Various cases of ghost images: Case 1) ghost reflection off SWFB then SWFA; Case 2) Ghost reflection off SWFB then SWPA; Case 3) Ghost reflection off COL3B then COL2B; Case 4) Ghost reflection off SW2B then SW1B; Case 5) Ghost reflection off Detector then SW2A.

As mentioned in the section 5.1 early, the NIRCam refractive system potentially has a ghost image counts of 15x14/2=105 for shortwave, and 17x16/2=136 for longwave. It is not necessary to analyze every ghost image. The ghost image is analyzed and screened based on the relative ghost magnitude. The ghost images with the largest magnitude are tabulated in Table 5 for shortwave, and Table 6 for longwave. In the Table 5 and 6, we have used the relative ghost magnitude of the center field for this category, since the ghost magnitude is the strongest at the center field comparing with corner fields.

Table 5: Ghost Image Analysis for Shortwave Channel

Reflection 1		Reflction 2		Ghost Image RMS Radius (mm)	Total Transmission for One Field	Relative Ghost Magnitude Per Pixel (Transmitted Energy/Pixel)	Ghost RMS Angular Diameter (arc second)	Ghost Reflection	Image Plane Footprint
Srf #	Name	Srf #	Name						
56	SWFB	53	SWFA	8.90E-03	1.30E-04	4.00E-03	0.03	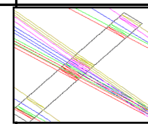	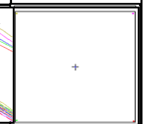
39	COL3A	38	COL2B	6.45E-03	5.27E-04	2.02E-03	0.02	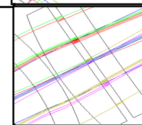	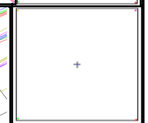
36	COL1B	35	COL1A	3.65E-01	1.71E-04	2.05E-07	1.29	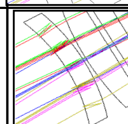	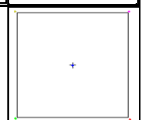
40	COL3B	38	COL2B	1.20E+01	2.34E-04	2.59E-10	42.31	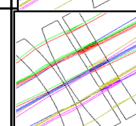	
40	COL3B	39	COL3A	1.20E+01	1.71E-04	1.90E-10	42.31	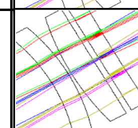	
NOMINAL				9.87E-03	6.11E-01	1.00E+00	0.03		

Table 6: Ghost Image Analysis for Longwave Channel

Reflection 1		Reflction 2		Ghost Image RMS Radius (mm)	Total Transmission for One Field	Relative Ghost Magnitude Per Pixel (Transmitted Energy/Pixel)	Ghost RMS Angular Diameter (arc second)	Ghost Reflection	Image Plane Footprint
Srf #	Name	Srf #	Name						
56	LWFB	53	LWFA	4.89E-03	8.15E-05	4.00E-03	0.03	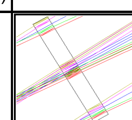	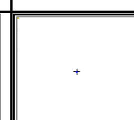
39	COL3A	38	COL2B	5.43E-03	6.24E-04	7.14E-04	0.04	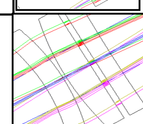	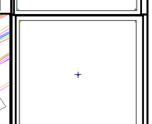
43	DBS2	42	DBS1	1.97E-02	6.90E-04	2.40E-04	0.14	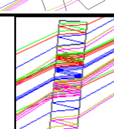	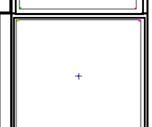
36	COL1B	35	COL1A	1.97E-01	2.03E-04	1.77E-07	1.39	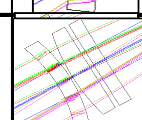	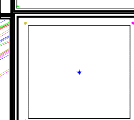
61	LW2A	39	CLO3A	5.66E-01	1.66E-05	1.75E-09	3.99	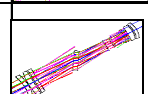	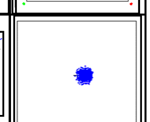
NOMINAL				4.94E-03	7.23E-01	1.00E+00	0.03		

5.3. Summary of Ghost Image Analysis

Most of the ghost images have a point spread function diameter greater than 1 arcsecond. Even though a few ghost images have an RMS angular diameter smaller than 1 arcsecond, their integrated flux is less than 1% of the nominal image. In summary, the requirement for ghost images is satisfied.

6. CONCLUSION

We have introduced the Compound Reflectance concept for the coating reflectance requirement of bandpass filter in order to reduce the ghost image at focal plane. The Compound Reflectance can be applied to other optical element to reduce the ghost image when the ghost image is a concern for an optical system. In this paper, NIRCam optical analysis has focused on three areas: vignetting analysis, alignment sensitivity and ghost image analysis. Results of the vignetting analysis indicate that vignetting is not an issue for the image path, and there is only minor throughput loss attributed to vignetting in the coronagraphic path. The sensitivity analysis has shown that the NIRCam instrument can be built and operated with reasonable and realizable alignment tolerances. The ghost image analysis has shown that NIRCam system meets the ghost image requirement.

Acknowledgment: Development of the NIRCam instrument at the Lockheed Martin Advanced Technology Center is performed under contract to and teamed with the University of Arizona's Steward Observatory. The University of Arizona in turn is under contract to the JWST Project at the NASA Goddard Space Flight Center.

Reference:

1. L. G. Burriesci, "NIRCam instrument overview", Proceeding of SPIE vol. 5904, 2005 (Presentation 5904-03).
2. ZEMAX is registered trademark of ZEMAX Development Corporation.
3. JWST NASA web site http://www.jwst.nasa.gov/.
4. L. W. Huff, "JWST NIRCam optics", Proceeding of SPIE vol. 5904, 2005 (Presentation 5904-04).